EXTENDED PDF FORMAT
SPONSORED BY
usb®
www.usbweb.com

Oxygen-18 of O2 Records the Impact of Abrupt Climate Change on the Terrestrial Biosphere

Jeffrey P. Severinghaus, *et al.*

Science **324**, 1431 (2009);
DOI: 10.1126/science.1169473

The following resources related to this article are available online at www.sciencemag.org (this information is current as of June 11, 2009):

Updated information and services, including high-resolution figures, can be found in the online version of this article at:
http://www.sciencemag.org/cgi/content/full/324/5933/1431

Supporting Online Material can be found at:
http://www.sciencemag.org/cgi/content/full/324/5933/1431/DC1

This article **cites 33 articles**, 5 of which can be accessed for free:
http://www.sciencemag.org/cgi/content/full/324/5933/1431#otherarticles

This article appears in the following **subject collections**:
Atmospheric Science
http://www.sciencemag.org/cgi/collection/atmos

Information about obtaining **reprints** of this article or about obtaining **permission to reproduce this article** in whole or in part can be found at:
http://www.sciencemag.org/about/permissions.dtl

Downloaded from www.sciencemag.org on June 11, 2009

Science (print ISSN 0036-8075; online ISSN 1095-9203) is published weekly, except the last week in December, by the American Association for the Advancement of Science, 1200 New York Avenue NW, Washington, DC 20005. Copyright 2009 by the American Association for the Advancement of Science; all rights reserved. The title *Science* is a registered trademark of AAAS.

sites, electrons can be injected into this network, and their propagation in the network could be observed with NC-AFM as described above. While STM is not ideally suited for this purpose because it relies on the tunneling of electrons (the unintended charging caused by the measurement and discharging of the structures via the substrate constitute a problem in STM experiments), we have shown that electrostatic AFM can enable the investigation of the charge landscape and of charge transport in metal-molecular nanostructures with atomic resolution.

References and Notes

1. Y. Sugimoto *et al.*, *Nature* **446**, 64 (2007).
2. Y. Sugimoto *et al.*, *Nat. Mater.* **4**, 156 (2005).
3. Y. Sugimoto *et al.*, *Science* **322**, 413 (2008).
4. M. Ternes, C. P. Lutz, C. F. Hirjibehedin, F. J. Giessibl, A. J. Heinrich, *Science* **319**, 1066 (2008).
5. M. Nonnenmacher, M. P. O'Boyle, H. K. Wickramasinghe, *Appl. Phys. Lett.* **58**, 2921 (1991).
6. S. Kitamura, K. Suzuki, M. Iwatsuki, C. B. Mooney, *Appl. Surf. Sci.* **157**, 222 (2000).
7. K. Okamoto, Y. Sugawara, S. Morita, *Appl. Surf. Sci.* **188**, 381 (2002).
8. M. Ikeda, N. Koide, L. Han, A. Sasahara, H. Onishi, *J. Phys. Chem. C* **112**, 6961 (2008).
9. G. H. Enevoldsen, T. Glatzel, M. C. Christensen, J. V. Lauritsen, F. Besenbacher, *Phys. Rev. Lett.* **100**, 236104 (2008).
10. F. Bocquet, L. Nony, C. Loppacher, T. Glatzel, *Phys. Rev. B* **78**, 035410 (2008).
11. K. Uchida, in *Nanoelectronics and Information Technology: Advanced Electronic Materials and Novel Devices*, R. Waser, Ed. (Wiley, New York, 2003), chap. 16.
12. K. K. Likharev, *IEEE Proc.* **87**, 606 (1999).
13. M. Haruta, *Catal. Today* **36**, 153 (1997).
14. J. Repp, G. Meyer, F. E. Olsson, M. Persson, *Science* **305**, 493 (2004).
15. F. E. Olsson, S. Paavilainen, M. Persson, J. Repp, G. Meyer, *Phys. Rev. Lett.* **98**, 176803 (2007).
16. M. Sterrer *et al.*, *Phys. Rev. Lett.* **98**, 096107 (2007).
17. C. Schoenenberger, S. F. Alvarado, *Phys. Rev. Lett.* **65**, 3162 (1990).
18. L. J. Klein, C. C. Williams, *Appl. Phys. Lett.* **79**, 1828 (2001).
19. R. Stomp *et al.*, *Phys. Rev. Lett.* **94**, 056802 (2005).
20. J. Zhu, M. Brink, P. L. McEuen, *Appl. Phys. Lett.* **87**, 242102 (2005).
21. E. Bussmann, N. Zheng, C. C. Williams, *Appl. Phys. Lett.* **86**, 163109 (2005).
22. E. Bussmann, C. C. Williams, *Appl. Phys. Lett.* **88**, 263108 (2006).
23. Y. Azuma, M. Kanehara, T. Teranishi, Y. Majima, *Phys. Rev. Lett.* **96**, 016108 (2006).
24. F. J. Giessibl, *Rev. Mod. Phys.* **75**, 949 (2003).
25. F. J. Giessibl, *Appl. Phys. Lett.* **76**, 1470 (2000).
26. Materials and methods are available as supporting material on *Science* Online.
27. T. Albrecht, P. Grütter, D. Horne, D. Rugar, *J. Appl. Phys.* **69**, 668 (1991).
28. J. E. Sader, S. P. Jarvis, *Appl. Phys. Lett.* **84**, 1801 (2004).
29. We observed that the LCPD and Δf^* are crucially dependent on the tip. However, the direction of the observed shifts in the LCPD and in Δf^* because of the atoms' charge state are not tip-dependent, allowing the determination of the charge states by comparison. In general, we observed higher shifts in the LCPD for smaller tip-sample separations and for tips exhibiting a small background force (that is, presumably very sharp tips).
30. We thank R. Allenspach for valuable comments. This work was supported by the Swiss National Center of Competence in Research (NCCR) "Nanoscale Science" and by the European Union project "NanoMan." P.L. and J.R. gratefully acknowledge funding by the Nederlandse Organisatie voor Wetenschappelijk Onderzoek (Chemical Sciences, Vidi-grant 700.56.423) and Volkswagen Foundation through its Lichtenberg program, respectively.

Supporting Online Material
www.sciencemag.org/cgi/content/full/324/5933/1428/DC1
Materials and Methods
SOM Text
Figs. S1 and S2
References

13 February 2009; accepted 1 May 2009
10.1126/science.1172273

Oxygen-18 of O_2 Records the Impact of Abrupt Climate Change on the Terrestrial Biosphere

Jeffrey P. Severinghaus,[1]* Ross Beaudette,[1] Melissa A. Headly,[1]† Kendrick Taylor,[2] Edward J. Brook[3]

Photosynthesis and respiration occur widely on Earth's surface, and the $^{18}O/^{16}O$ ratio of the oxygen produced and consumed varies with climatic conditions. As a consequence, the history of climate is reflected in the deviation of the $^{18}O/^{16}O$ of air ($\delta^{18}O_{atm}$) from seawater $\delta^{18}O$ (known as the Dole effect). We report variations in $\delta^{18}O_{atm}$ over the past 60,000 years related to Heinrich and Dansgaard-Oeschger events, two modes of abrupt climate change observed during the last ice age. Correlations with cave records support the hypothesis that the Dole effect is primarily governed by the strength of the Asian and North African monsoons and confirm that widespread changes in low-latitude terrestrial rainfall accompanied abrupt climate change. The rapid $\delta^{18}O_{atm}$ changes can also be used to synchronize ice records by providing global time markers.

The mechanism of abrupt climate change, in particular the Heinrich and Dansgaard-Oeschger (D/O) events of the last ice age, remains poorly understood (*1*). One barrier is the dearth of information about the spatial extent of the events, due in part to the paucity of low-latitude paleoclimate records with sufficient dating precision to establish whether events are synchronous, time-transgressive, or unrelated (*2*). Cave stalagmite $\delta^{18}O$ records with radiometric U/Th dating are a notable exception (*3*–*6*), but these are still spot records with generally unknown spatial importance. Atmospheric gas records from ice cores can help address the spatial issue because the atmosphere acts as an integrator of innumerable gas fluxes over broad spatial scales. Methane has been used in this capacity (*7*), but methane production is dominated by rather special settings (e.g., high-productivity anoxic wetland soils). Oxygen (O_2), in contrast, is produced widely in the low latitudes by photosynthesis, making it a more ideal tracer of the spatial extent and global importance of climate change. In particular, the isotopic composition of oxygen produced on land varies strongly with environmental conditions, making it a unique tracer of the impact of climate on the terrestrial biosphere (*8*–*11*).

The $^{18}O/^{16}O$ ratio of atmospheric molecular oxygen ($\delta^{18}O_{atm}$) is known to vary on orbital time scales in response to the growth of ice sheets and changes in biogeochemical fractionation (*8*–*11*), with a typical glacial-interglacial range of ~1.5 per mil (‰). The substrate for all photosynthetic oxygen production is water, and the isotopic composition of the water ($H_2{}^{18}O/H_2{}^{16}O$) in which photosynthesis occurs is transferred to O_2 (*12*). Thus, variations in water $\delta^{18}O$ at the site of photosynthesis (i.e., the chloroplast) are a primary cause of variation in $\delta^{18}O_{atm}$ (*13*). Ice sheet growth and decay, with attendant change in seawater $\delta^{18}O$ (and thus all meteoric water), causes roughly half of the variation. The balance is due to changes in hydrological cycle fractionation during condensation and evaporation that affect chloroplast water $\delta^{18}O$, and fractionation by the respiratory sink of O_2 (*10*, *11*). These fractionation processes collectively create a steady-state offset between seawater $\delta^{18}O$ and the $\delta^{18}O$ of O_2, known as the Dole effect, which today amounts to +23.88‰ (*14*).

Past variations in the Dole effect are known to occur on orbital time scales, chiefly the 23,000-year (23 ky) precession period (*10*, *11*). These variations are likely due to the Asian and African monsoon variations that occur on this time scale because of the impact of precession on summer insolation (*15*, *16*), although other factors may also contribute, and the subject is currently not well understood. Faster variations have generally not been expected because of the ~1000-year turnover time of atmospheric O_2.

---

[1] Scripps Institution of Oceanography, University of California, San Diego, CA 92093–0244, USA. [2] Desert Research Institute, Nevada System of Higher Education, 2215 Raggio Boulevard, Reno, NV 89512, USA. [3] Department of Geosciences, Oregon State University, Corvallis, OR 97331, USA.

*To whom correspondence should be addressed. E-mail: jseveringhaus@ucsd.edu

†Present address: The Pennington School, 112 West Delaware Avenue, Pennington, NJ 08534, USA.

This view was challenged by recent high-precision and high-resolution measurements in the North Greenland Ice Core Project (NGRIP) ice core between 60,000 and 75,000 years ago (60 to 75 ka), which showed rapid millennial-scale variations in $\delta^{18}O_{atm}$ (*17*). Here, we extend this finding to the complete 0- to 100-ka interval with a new $\delta^{18}O_{atm}$ record from the Siple Dome ice core, Antarctica, and a short record (24 to 14 ka) from the Greenland Ice Sheet Project 2 (GISP2) ice core, Greenland. We analyzed samples in duplicate for $\delta^{15}N$, $\delta^{18}O$ of O_2, $\delta O_2/N_2$, and $\delta Ar/N_2$ following established procedures (*18*–*20*). We use the customary notation $\delta^{18}O = [(^{18}O^{16}O/^{16}O_2)_{sample}/(^{18}O^{16}O/^{16}O_2)_{reference} - 1]$‰, and the reference for all four measured gases is the modern atmosphere in La Jolla in 2006.

In addition to the previously known orbital variation, the new $\delta^{18}O_{atm}$ record shows variations on the millennial scale (Fig. 1). Their appearance in multiple ice core records confirms that they are real atmospheric features and not artifacts (*19*).

Prominent cold periods in the Northern Hemisphere known as Heinrich stadials (*21*, *22*) appear as positive anomalies of ~0.15‰ in $\delta^{18}O_{atm}$, or positive changes in the derivative (Fig. 1; note that the $\delta^{18}O_{atm}$ scale is inverted, following convention). Generally, the signature of the cold stadial phases of the D/O events (termed D/O stadials) is more muted but still recognizable, especially for the longer events (Fig. 2).

To further explore the isotopic fluxes from land to atmosphere and associated climatic changes, we take the derivative of the data and account for the effects of oceanic processes. Because the ~1000-year turnover time of O_2 in the atmosphere acts as an integrator, imparting a smoothing to the record of isotopic fluxes to the atmosphere, we remove the smoothing effect with a one-box model deconvolution (*19*).

$$\Delta\varepsilon_{LAND} = \left[\tau\frac{d\delta_{atm}}{dt} + \delta_{atm} - \delta_{seawater}\right]\frac{1}{f_L} \qquad (1)$$

Here, $\Delta\varepsilon_{LAND}$ is an empirical parameter that represents the lumped changes over time in the terrestrial hydrological and respiratory fractionations that create the changes in the Dole effect, τ is the turnover time of 1000 years, the derivative is calculated from a least-squares Fourier-series fit to the $\delta^{18}O_{atm}$ time series data, $\delta_{seawater}$ is an estimate of seawater $\delta^{18}O$ through time (*23*), and f_L is the fraction of total oxygenesis occurring on land (taken to be 0.65) (*19*). Although it is unlikely that f_L is constant in time, we neglect changes in f_L based on recent findings that the intrinsic fractionation of terrestrial and oceanic processes contributing to the Dole effect are more similar than previously believed (*24*–*27*), so variations in their relative oxygen production will have little influence on the Dole effect.

We urge caution in interpreting the fractionation parameter $\Delta\varepsilon_{LAND}$, because the seawater $\delta^{18}O$ curve is highly smoothed in comparison to our high-frequency $\delta^{18}O_{atm}$ curve. This could have the effect of creating spurious changes in $\Delta\varepsilon_{LAND}$ during stadials (if the smoothing has removed a positive anomaly in seawater $\delta^{18}O$) or an underestimate of the amplitude of the millennial-scale positive anomalies in $\Delta\varepsilon_{LAND}$ (if the smoothing has removed a negative anomaly in seawater $\delta^{18}O$). We argue that the latter possibility is the

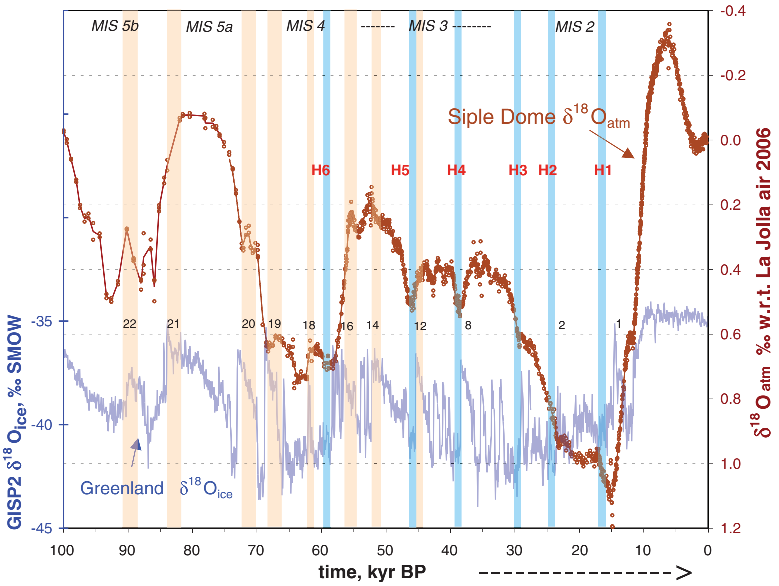

Fig. 1. Measured $^{18}O/^{16}O$ of atmospheric molecular oxygen ($\delta^{18}O_{atm}$) over the past 100 ky from the Siple Dome ice core, Antarctica (note inverted right axis). Data have been corrected for gravitational settling in the firn layer on top of the ice sheet using measured $\delta^{15}N$ and for gas-loss–induced fractionation using measured $\delta O_2/N_2$ and $\delta Ar/N_2$ (*19*). The line drawn through points from 0 to 75 ka is a least-squares fit, and the line from 75 to 100 ka connects mean values. Approximate timings of the marine isotope stages (MISs) are shown at the top. Greenland $\delta^{18}O_{ice}$ (*40*) is shown for reference, and Heinrich stadials (H1 to H6 in red numbers) and the older D/O events (small black numbers) are labeled. Time scale is synchronized to GISP2 (*41*).

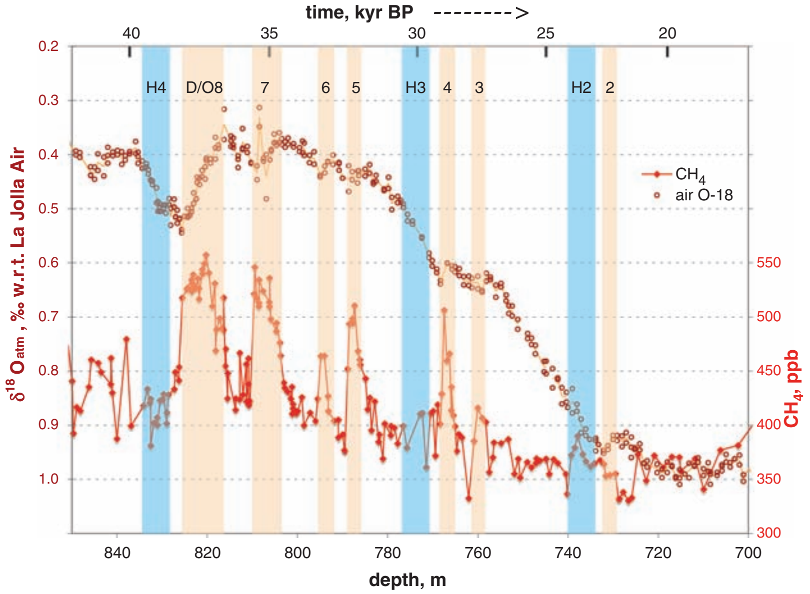

Fig. 2. Expanded view of $\delta^{18}O_{atm}$ from the Siple Dome ice core during D/O events of MIS 3, plotted versus depth to show the raw temporal relationship to methane (measured in the same ice core), without further complications from gas age assignment. Individual $\delta^{18}O_{atm}$ replicates shown, with means connected by solid line. Inferred positions of Heinrich stadials (H4 to H2) and D/O events (D/O8 to D/O2) are shown with vertical shaded bars. Approximate ages are given at top. Methane data from (*41*).

more likely one, because Heinrich stadial 1 is clearly accompanied by rising sea level, and therefore decreasing seawater δ^{18}O (*28*, *29*). By analogy to Heinrich stadial 1, we argue that all Heinrich stadials are accompanied by negative seawater δ^{18}O anomalies, making our deduced positive Dole effect anomalies at these times minimum estimates.

If respiratory fractionation were constant (not necessarily realistic), $\Delta\varepsilon_{LAND}$ would be equal to the isotopic fractionation of terrestrial chloroplast water relative to seawater (strictly, production-weighted-mean terrestrial chloroplast water δ^{18}O minus seawater δ^{18}O). In this case, $\Delta\varepsilon_{LAND}$ would give globally integrated information about the hydrological cycle, in particular the δ^{18}O of precipitation over photosynthetically active land areas such as the monsoon regions, and the relative humidity in these areas [which controls the amount of evaporative enrichment of the leaf water δ^{18}O (*10*, *13*)]. Strong summer monsoons affect both mechanisms in the same sense, with less isotopic enrichment (*10*, *11*, *15*, *16*).

The good correlation between $\Delta\varepsilon_{LAND}$ and independent indicators of monsoon strength from Chinese cave records (Fig. 3) lends support to the view that the Dole effect is tightly linked to the strength of the Asian monsoon (*10*, *15*, *16*). Detailed correlations during the last deglaciation and the Holocene lend further support to this view (r = 0.95) (*30*) and even suggest coherence at centennial time scales (Fig. 4). The fact that the abrupt climate event at 8.2 ka has a visible impact on the Dole effect (Fig. 4) is noteworthy because of its short duration and lack of seawater δ^{18}O change. The rapidity of the changes in δ$^{18}O_{atm}$ are surprising and raise the question of whether the turnover time of oxygen in the atmosphere has been overestimated, pointing to the need for further work.

Changes in respiration over time may also have contributed to the variations in the Dole effect, although understanding is limited at present. Respiration increases closely in parallel with increases in photosynthesis, and strong monsoons might be expected to increase the global proportion of weakly fractionating tropical respiration (~10‰) relative to boreal respiration (~22‰), which could be a powerful effect (*26*). Again, the fractionation change would be in the same sense (more tropical respiration causes a decrease in δ$^{18}O_{atm}$ and $\Delta\varepsilon_{LAND}$) as that caused by precipitation. Thus, part of the correlation between $\Delta\varepsilon_{LAND}$ and monsoon strength could be due to respiration; we therefore caution against using $\Delta\varepsilon_{LAND}$ as a proxy for chloroplast water δ^{18}O.

The implication of these data is that a very large, albeit poorly quantified, fraction of the photosynthetic capacity of the planet's terrestrial surface was affected by Heinrich and D/O stadials. As noted above, a similar conclusion has been drawn from the ice core methane record (*31*). However, methane production takes place in anoxic soils, prevalent only in wetland regions, whereas oxygen is produced widely over the land surface. Thus, our data strengthen conclusions about the involvement of the low-latitude hydrological cycle in abrupt climate change that were already drawn from ice core methane data (*7*, *31*) and local records (*32*).

These findings are consistent with recent speleothem records (*6*) and modeling results (*33*, *34*) that suggest that the intertropical convergence zone (ITCZ) can abruptly shift to a state in which it stays predominantly in the southern hemisphere during Heinrich and D/O stadials. Because of the paucity of land in the southern hemisphere, and the fact that rainfall on the ocean has little effect on marine chloroplast water δ^{18}O due to dilution by seawater, a southern-shifted ITCZ is expected to produce high $\Delta\varepsilon_{LAND}$ and a strong Dole effect. Also, the ITCZ stimulates vigorous plant growth on the land that does exist in the southern hemisphere. A southern-shifted locus of intense oxygenesis should strengthen the Dole effect, because the δ^{18}O of terrestrial oxygenic precipitation in the Southern Hemisphere is generally higher than in the Northern Hemisphere because of lesser continentality, lower altitude, and less intense isotopic distillation, as suggested by the fact that Southern Hemisphere Brazilian cave records are ~4‰ higher in δ^{18}O during corresponding phases than their Chinese counterparts (*6*).

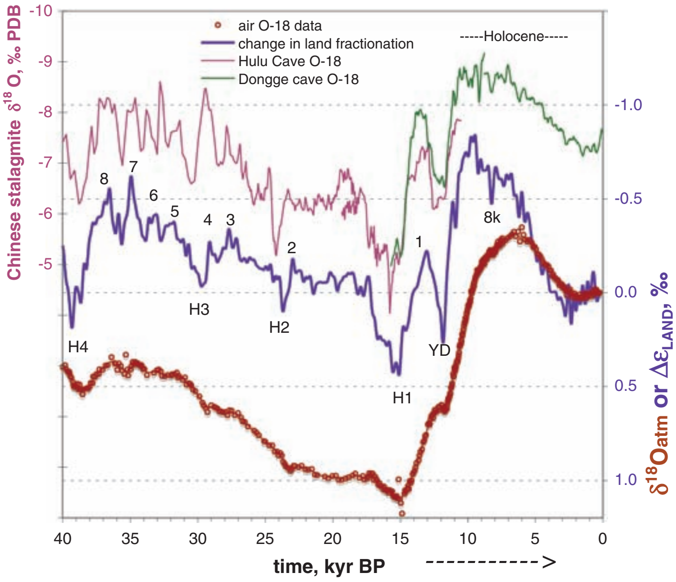

Fig. 3. Records over the past 40 ky of $^{18}O/^{16}O$ of atmospheric molecular oxygen (δ$^{18}O_{atm}$), inferred change in terrestrial $^{18}O/^{16}O$ fractionation ($\Delta\varepsilon_{LAND}$), and Chinese cave stalagmite $^{18}O/^{16}O$ (*3*–*5*). Dongge Cave records are smoothed with a 200-year moving average for clarity (*30*). D/O events 2 to 8 and Heinrich stadials H1 to H4 are numbered, and Younger Dryas (YD) and 8.2-ka event (8k) are labeled.

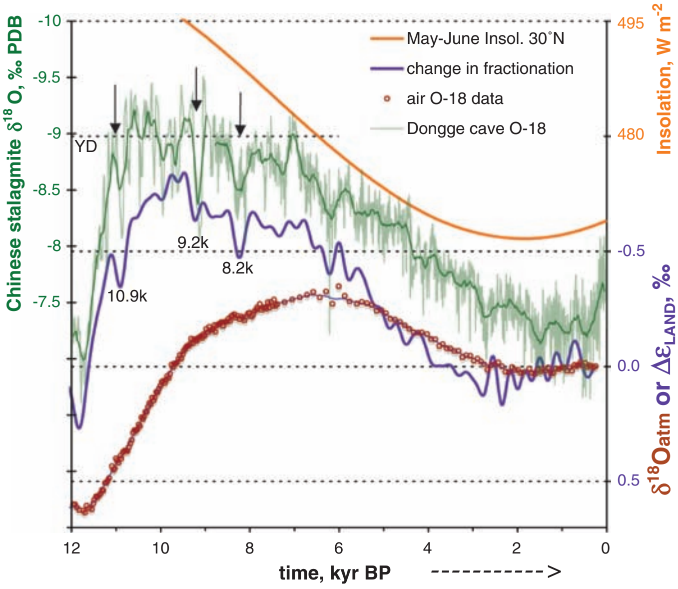

Fig. 4. Expanded view of Holocene portion of Fig. 3. Similarities between inferred global terrestrial $^{18}O/^{16}O$ fractionation ($\Delta\varepsilon_{LAND}$) and the Chinese cave $^{18}O/^{16}O$ are noted with arrows at 8.2 ka, 9.2 ka, and 10.9 ka (8.2k, 9.2k, and 10.9k, respectively). Dongge cave records (*4*, *5*) are shown raw and with a 200-year running average and have been corrected for seawater $^{18}O/^{16}O$ change (*23*) to emphasize the fractionation relative to seawater. The upturn in monsoon strength around 2 ky before the present (BP) implied by $\Delta\varepsilon_{LAND}$ could have been driven by the upturn in May and June mean insolation (*42*), suggesting that there is no need to invoke an anthropogenic cause (*43*) of the upturn in atmospheric methane concentration at that time.

We cannot rule out a small role of boreal ecosystems in shaping $\Delta\varepsilon_{LAND}$, because photosynthesis in these latitudes would be expected to produce isotopically light O_2 from snowmelt during warm phases of the D/O events. We also cannot rule out the hypothesis (*17*) that lower relative humidity over most land areas and a southward-shifted vegetation distribution explains the strong Dole effect during D/O stadials. However, the temporal pattern of $\Delta\varepsilon_{LAND}$ (strong Heinrich and weak D/O stadials, abrupt mid-Holocene change) (Figs. 3 and 4) does not match that of known boreal climate patterns (e.g., weak Heinrich and strong D/O, a steady Holocene cooling) (Fig. 1). Also, the strong boreal respiratory fractionation (*26*) should nullify the effect of boreal photosynthesis to some extent (*35*). We thus suggest that our $\delta^{18}O_{atm}$ data imply large changes in low-latitude terrestrial hydrology associated with abrupt climate change, whether (i) directly through the low $\delta^{18}O$ of heavy precipitation, (ii) indirectly through the weak evaporative enrichment of chloroplast water under conditions of high humidity, or (iii) indirectly through the weak respiratory fractionation that characterizes wet tropical biomes. These findings highlight in a general way the sensitivity of low-latitude rainfall patterns to abrupt climate change in the high-latitude north, with possible relevance for future rainfall and agriculture in the heavily populated monsoon regions.

Finally, the millennial scale oscillations in $\delta^{18}O_{atm}$ open up possibilities for improving the dating of ice cores and glacial outcrops. Because the atmosphere is well-mixed on 1-year time scales, $\delta^{18}O_{atm}$ is a global time-stratigraphic marker that has been used for synchronizing different ice core chronologies (*36*). Previous use of $\delta^{18}O_{atm}$ has been limited to the orbital scale, however, and millennial-scale dating has been done with methane concentration (*37*). During times when methane concentration varied little, such as during the last glacial maximum, the small variations in $\delta^{18}O_{atm}$ that we identify provide new tie points (e.g., fig. S5). Also, low-latitude ice cores generally do not preserve reliable atmospheric methane records because methane is a trace gas that is vulnerable to in situ production (*38*). As an abundant gas, oxygen is more resistant to in situ alteration, making $\delta^{18}O_{atm}$ useful for millennial-scale dating of low-latitude ice cores.

References and Notes

1. G. H. Denton, R. B. Alley, G. C. Comer, W. S. Broecker, *Quat. Sci. Rev.* **24**, 1159 (2005).
2. C. Wunsch, *Quat. Sci. Rev.* **22**, 1631 (2003).
3. Y. J. Wang *et al.*, *Science* **294**, 2345 (2001).
4. Y. J. Wang *et al.*, *Science* **308**, 854 (2005).
5. C. A. Dykoski *et al.*, *Earth Planet. Sci. Lett.* **233**, 71 (2005).
6. X. Wang *et al.*, *Geophys. Res. Lett.* **34**, L23701 10.1029/2007GL031149 (2007).
7. E. J. Brook, S. Harder, J. Severinghaus, E. J. Steig, C. M. Sucher, *Global Biogeochem. Cycles* **14**, 559 (2000).
8. T. Sowers, M. L. Bender, D. Raynaud, *J. Geophys. Res.* **94**, 5137 (1989).
9. M. Bender *et al.*, *Nature* **372**, 663 (1994).
10. M. L. Bender, T. Sowers, L. Labeyrie, *Global Biogeochem. Cycles* **8**, 363 (1994).
11. B. Malaizé, D. Paillard, J. Jouzel, D. Raynaud, *J. Geophys. Res.-Atmos.* **104**, 14199 (1999).
12. R. D. Guy, M. L. Fogel, J. A. Berry, *Plant Physiol.* **101**, 37 (1993).
13. G. D. Farquhar, L. A. Cernusak, B. Barnes, *Plant Physiol.* **143**, 11 (2007).
14. E. Barkan, B. Luz, *Rapid Commun. Mass Spectrom.* **19**, 3737 10.1002/rcm.2250 (2005).
15. M.-A. Mélières, M. Rossignol-Strick, B. Malaizé, *Geophys. Res. Lett.* **24**, 1235 (1997).
16. V. Masson *et al.*, *Geophys. Res. Lett.* **27**, 1747 (2000).
17. A. Landais *et al.*, *Earth Planet. Sci. Lett.* **258**, 101 (2007).
18. V. V. Petrenko, J. P. Severinghaus, E. J. Brook, N. Reeh, H. Schaefer, *Quat. Sci. Rev.* **25**, 865 (2006).
19. Materials and methods are available as supporting material on *Science* Online.
20. Electronic archived data is available at http://gcmd.nasa.gov/getdif.htm?0440975_severinghaus.
21. S. Barker *et al.*, *Nature* **457**, 1097 (2009).
22. We believe that it is useful to make a distinction between stadials with an associated Heinrich event (Heinrich stadials) and those without (D/O stadials). In the tropics, Heinrich stadials have a different character than D/O stadials, suggesting a different mechanism. The amplitude of the former in the tropics is larger than that of the D/O stadials, in contrast to high-latitude records, where all stadials seem to have a similar expression. It has been proposed (*39*) that the Heinrich stadials represent times when the Atlantic meridional overturning circulation was completely shut off, and the D/O stadials represent times when only the Greenland-Iceland-Norwegian (GIN) seas and the associated overflows on the Greenland-Scotland ridge were shut off, with the Labrador Sea continuing to produce deep water. The implication of this hypothesis is that the northward cross-equatorial flow in the Atlantic ceased during Heinrich stadials but not during the D/O stadials. This could explain why the two types of events seem so different in the low latitudes, because near-equatorial meridional sea surface temperature gradients (e.g., 20°N to 20°S) have a profound effect on the mean position of the ITCZ (*33*).
23. C. Waelbroeck *et al.*, *Quat. Sci. Rev.* **21**, 295 (2002).
24. M. Hendricks, M. L. Bender, B. Barnett, *Deep Sea Res. Part I Oceanogr. Res. Pap.* **51**, 1541 (2004).
25. E. Barkan, D. Eisenstadt, A. Kaplan, B. Luz, The effect of marine photosynthesis on $^{17}O/^{16}O$ and $^{18}O/^{16}O$ of atmospheric O_2 (abstr.), Proceedings Goldschmidt 2009, Davos, 21 to 26 June 2009.
26. A. Angert *et al.*, *Global Biogeochem. Cycles* **17**, 1089 10.1029/2003GB002056 (2003).
27. The idea that the fraction of land versus ocean photosynthesis influences the Dole effect is awkward in its construction; it implicitly assumes that there is a single "land" value of fractionation, whereas in fact it is now clear that the land fractionation is extremely heterogeneous in time and space. It may be conceptually more helpful to think of the Dole effect as being the integral of competing "heavy" land isofluxes (e.g., from savannas, deserts, and well-aerated soils) and "light" land isofluxes (e.g., from humid, water-saturated biomes), against a background of relatively uniform and constant oceanic values. (Here, the concept of isofluxes subsumes the isotopic effects of both sources and sinks.)
28. G. H. Denton, W. S. Broecker, R. B. Alley, *PAGES News* **14**, 1416 (2006).
29. The view that Heinrich stadials are times of sea-level rise is supported by speleothem records (*32*) that show a consistent pattern of weak monsoons during times of sea-level rise at many glacial terminations, suggesting that there is some unifying mechanism that produces Heinrich-like stadials and weak monsoons in the presence of sea level rise. For example, such a mechanism could be the effect of meltwater injected into the North Atlantic ocean on the meridional ocean overturning circulation and winter sea ice cover in the North Atlantic (*1*).
30. A composite Dongge Cave record was constructed from the entire 8.8-ky record of Wang *et al.* (*4*) and the Dongge D4 record (*5*) from 8.8 to 15.7 ka, and was linearly interpolated and smoothed with a 200-year running average (Fig. 3). This average was resampled at 20-year intervals for comparison with $\Delta\varepsilon_{LAND}$, giving a Pearson correlation coefficient (*r*) of 0.95 for the 0.3- to 12-ka interval (Fig. 4). The correlation between $\Delta\varepsilon_{LAND}$ and Hulu Cave records is visually apparent but numerically limited by time scale errors (GISP2 time scale is up to 1 ky too young in the 16- to 31-ka interval).
31. J. Chappellaz *et al.*, *Nature* **366**, 443 (1993).
32. Y. J. Wang *et al.*, *Nature* **451**, 1090 (2008).
33. J. C. H. Chiang, C. M. Bitz, *Clim. Dyn.* 10.1007/s00382-005-0040-5 (2005).
34. J. C. H. Chiang, W. Cheng, C. M. Bitz, *Geophys. Res. Lett.* **35**, L07704 10.1029/2008GL033292 (2008).
35. The amount of photosynthesis occurring in boreal regions is known to increase during the warm phases of D/O events (from pollen records). The amount of respiration must also increase at these times, because respiration and photosynthesis are tightly coupled by the fact that organic matter is generally unstable with respect to microbial attack. Thus, the respiratory contribution to the Dole effect will increase because the boreal respiratory fractionation factor is greater than the mean global value. The same logic holds in reverse for wet tropical biomes, in the Asian and African monsoon regions. Here, weak respiratory fractionation has the effect of reducing the Dole effect when wet tropical oxygenesis/respiration increases during warm phases of D/O events, even if the magnitude of the fractionation in that biome is constant. The key point is that respiration and hydrological-fractionation-with-oxygenesis have opposing effects in boreal biomes but constructive effects in tropical biomes. Therefore, wet tropical biomes should dominate the variability in the Dole effect, rather than boreal biomes, because of this "monsoon rectifier effect."
36. M. L. Bender, B. Malaizé, J. Orchardo, T. Sowers, J. Jouzel, in *Mechanisms of Global Climate Change at Millennial Time Scales*, P. U. Clark, R. S. Webb, L. D. Keigwin, Eds., vol. 112, *Geophysical Monograph Series* (American Geophysical Union, Washington, DC, 1999), pp. 149–164.
37. T. Blunier, E. J. Brook, *Science* **291**, 109 (2001).
38. R. K. Campen, T. Sowers, R. B. Alley, *Geology* **31**, 231 (2003).
39. R. B. Alley, P. U. Clark, L. D. Keigwin, R. S. Webb, in *Mechanisms of Global Change at Millennial Time Scales*, P. U. Clark, R. S. Webb, L. D. Keigwin, Eds., vol. 112, *Geophysical Monograph Series* (American Geophysical Union, Washington, DC, 1999), pp. 385–394.
40. M. Stuiver *et al.*, *Quat. Res.* **44**, 341 (1995).
41. E. J. Brook *et al.*, *Quat. Sci. Rev.* **24**, 1333 (2005).
42. D. Paillard, L. Labeyrie, P. Yiou, *Eos Trans. AGU* **77**, 379 (1996).
43. W. F. Ruddiman, *Clim. Change* **61**, 261 (2003).
44. We thank B. Luz, L. Edwards, R. Keeling, M. Bender, A. Landais, K. Kawamura, C. Wunsch, G. Farquhar, and W. Broecker for helpful conversations. B. Cornuelle did the Fourier-series curve fitting. M. Henkart analyzed the tank of air from 1976 to test for anthropogenic change in the Dole effect. We thank J. Rhoades and the staff of the National Ice Core Laboratory for help in sampling the Siple Dome ice core. This work was supported by NSF-OPP 04-40975 (J.P.S), NSF-OPP 01-26057 (E.J.B), and the Gary Comer Science and Education Foundation, and recovery of the Siple Dome ice core was supported by NSF-OPP 95-26421 (K.T.).

Supporting Online Material

www.sciencemag.org/cgi/content/full/324/5933/1431/DC1
Materials and Methods
Figs. S1 to S10
References

8 December 2008; accepted 30 April 2009
10.1126/science.1169473